DOI: 10.1002/ejoc.201100873

Irreversible Inhibition of Monoamine Oxidase B by the Antiparkinsonian Medicines Rasagiline and Selegiline: A Computational Study

Rok Borštnar,[a] Matej Repič,[a] Mojca Kržan,[b] Janez Mavri,[a,c] and Robert Vianello*[a,d]

Keywords: Medicinal chemistry / Molecular modeling / Enzymes / Inhibitors / Parkinson disease / Reaction mechanisms

We used quantum-chemical methods to study seven possible mechanisms of monoamine oxidase (MAO) inhibition by acetylenic inhibitors, considering neutral, cationic, anionic and radical mechanisms. MAO is a flavoenzyme responsible for the metabolism of the important neurotransmitters noradrenaline, serotonin and dopamine. It exists in two isoforms: MAO A and MAO B. Selective MAO A inhibitors are used in the treatment of depression, whereas selective MAO B inhibitors such as rasagiline and selegiline are used to relieve symptoms of Parkinson disease. Rasagiline and selegiline are irreversible MAO B inhibitors, each forming a covalent bond with the enzyme's flavin adenine dinucleotide (FAD) cofactor upon inhibition. Although widely used, they both exhibit numerous adverse effects. Our calculations, performed at the B3LYP/6-311++G(2d,2p)//B3LYP/6-31+G(d) level of theory, with application of the CPCM solvent reaction field with ε = 4 to mimic the polar environment, found that a polar anionic mechanism, involving deprotonation of the inhibitor molecule at the terminal acetylene carbon atom, is the most plausible. The calculated free energies of activation for rasagiline and selegiline by this mechanistic pathway are 19.9 and 23.7 kcal mol^{-1}, respectively, in very good agreement with experimentally determined values of 20.8 and 21.3 kcal mol^{-1}, respectively. Together with additional experimental and theoretical work, the results presented here could lead to better understanding of the nature of MAO inhibition and possible design of new antiparkinsonians as improved MAO B inhibitors. Some ideas on the strategy to achieve that and perspectives for future work are also given.

1. Introduction

Monoamine oxidases (MAOs) are flavoenzymes sited in the outer mitochondrial membranes of brain, liver, intestinal and placental cells and platelets, which catalyse the oxidation of a large variety of amine neurotransmitters into the corresponding imines.[1–4] Flavoenzymes typically contain either a flavin mononucleotide (FMN) or a flavin adenine dinucleotide (FAD) cofactor, noncovalently bound to the apoprotein.[5] In some flavoenzymes the isoalloxazine ring of the flavin is covalently linked to a His, Cys or Tyr residue of the polypeptide chain. In MAOs, FAD coenzyme is covalently bound in an 8α-thioether linkage to Cys397 (Scheme 1), which has been determined to be an absolute requirement for MAOs to work.[6,7] The enzyme exists in two isozymic forms – MAO A and MAO B[8] – that differ in substrate and inhibitor selectivity[9] as well as in tissue distribution.[10,11] MAO A is mainly responsible for the oxidation of noradrenaline and serotonin. Imbalances in noradrenaline/serotonin levels are known to cause depression-like symptoms[12,13] and other mood disorders. Selective inhibition of this isoform hence results in elevated noradrenaline and serotonin concentrations, thus gradually improving the symptoms of depression. In contrast, MAO B is responsible for the metabolism of the histamine metabolite *N*-methylhistamine and the important neurotransmitter dopamine.[14–16] The most characteristic feature of Parkinson disease is progressive cell death of dopaminergic neurons in the *pars compacta* of the brain's *substantia nigra*, affecting approximately 70% of cells when symptoms occur.[17] Inhibition of MAO B is therefore a crucial strategy for relief of symptoms of Parkinson disease.[16,18] Most MAO B inhibitors currently used as antiparkinsonians are irreversible:[19] that is, a covalent bond between the inhibitor and the enzyme is formed, preventing further activity of the enzyme.

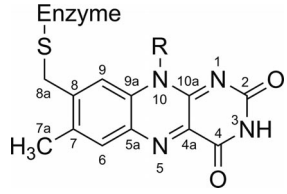

Scheme 1. Atom numbering of the flavin moiety responsible for the catalytic activity of MAO enzymes (R = adenosine diphosphate group).

[a] Laboratory for Biocomputing and Bioinformatics, National Institute of Chemistry,
Hajdrihova 19, 1000 Ljubljana, Slovenia
Fax: +386-1-4760300
E-mail: robert.vianello@irb.hr
[b] Department of Pharmacology and Experimental Toxicology, Faculty of Medicine, University of Ljubljana,
Korytkova 2, 1000 Ljubljana, Slovenia
[c] EN-FIST Centre of Excellence,
Dunajska 156, 1000 Ljubljana, Slovenia
[d] Quantum Organic Chemistry Group, Ruđer Bošković Institute,
Bijenička cesta 54, 10000 Zagreb, Croatia

There are two important structural features of MAO B that are worth noting for assessment of the catalytic/inhibition mechanism: its active site hydrophobicity and the conformation of the flavin.[20–24] The first characteristic is important for substrate access to the MAO active site, because MAO substrates are protonated in cytoplasm and exist as monocations under physiological conditions. Edmondson and co-workers[23] offered the explanation that, because the free energy cost associated with the translocation of a charged moiety into the hydrophobic active site would be too high, the substrate should enter the enzyme in its neutral form, although the exact mechanism of this initial deprotonation is not known. This is also one of the reasons why gas-phase calculations involving MAO active site might be quite reliable. With regard to the conformation of the flavin, structural analysis of rasagiline-inhibited MAO B[22] revealed the flavin moiety to be bent by ca. 30° from planarity around the axis connecting the nitrogen atoms N5 and N10 of the central ring (Scheme 1). As can be seen later, this structural feature of the flavin group could also be used in distinguishing between different MAO inhibition mechanisms in a qualitative way.

The elucidation of the three-dimensional structures of MAO A[25] and MAO B[20,26] isozymes allowed for investigation of the catalytic mechanism, which is of paramount importance for development of new inhibitors. Researchers have tried to interpret the substrate selectivity[23] on the basis of these structural features and have proposed several catalytic mechanisms. Moreover, extensive studies on mutant enzymes have been carried out in order to provide better understanding of the effect of the internal protein environment on MAO catalysis,[7,22,27] but despite huge efforts, there is at present no consensus on the actual mechanism of the catalytic step.

Three distinct mechanisms by which MAO might oxidize substrates have been proposed so far: 1) a hydride mechanism, 2) a radical mechanism, and 3) a polar nucleophilic mechanism. In other words, it is assumed that the catalytic rate-limiting step involves one out of heterolytic H^- abstraction in (1), or homolytic $H^\cdot$ extraction in (2), or deprotonation of H^+ in (3), all from the α-carbon atom of the substrate. Common to all mechanisms is that the activating stage mentioned is performed by the N5 atom on the flavin (Scheme 1), which is also the site of the irreversible inhibitor attack. Erdem et al.[28] assumed that the hydride mechanism is unlikely to take place, because hydride transfer is associated with a barrier too high to be readily crossed,[29] unlike in the amino acid oxidase[30–33] and alcohol oxidase[2,34,35] classes of flavoenzymes, for which hydride mechanisms are suggested. Studies by Miller and Edmondson[36] with benzylamine analogues showed that attachment of electron-withdrawing groups to the *para*-position of the benzylamine substrate increases the rate of the reaction in the case of MAO A, which provides strong experimental evidence that proton transfer, and not hydride anion abstraction, is an integral part of the rate-limiting step. On the basis of these kinetic and structural data, and the mentioned Taft correlation, the authors proposed the polar nucleophilic mechanism for MAO A,[36] although this has been disputed in the literature, mostly by Silverman and co-workers,[37–39] in favour of the radical mechanism. In contrast, the Miller and Edmondson study also found that this effect on the reaction rate is much less effective in the case of MAO B than in that of MAO A, opening up the possibility that the two isozymes do not function by the same mechanism. On the other hand, such different behaviour in MAO isozymes is in accordance with the radical mechanism proposed by Silverman and co-workers[40–44] in which the first step is the one-electron transfer from the substrate amino group to the flavin to form the substrate radical cation. However, subsequent experiments by Edmondson et al.,[23,45] as well as related electron paramagnetic resonance (EPR) studies[46] and stopped-flow kinetic determinations,[47,48] failed to provide evidence for any radical intermediates. In addition to that, no influence of magnetic field on the rate of enzyme reduction was observed.[49] A very probable explanation for kinetic differences between MAO A and MAO B with different substrates involves consideration of long-range preorganized electrostatics as the main factor responsible for the catalysis.[50] Another interesting aspect of the study by Miller and Edmondson worth noting is the large H/D kinetic isotope effect (KIE) of 6–14 determined for MAO B catalysis.[7,36,51–53] Such a large KIE effect exceeds the contribution of zero-point energy and can be attributed to tunnelling. Still, the detailed mechanism of flavin-dependent amine oxidation remains a subject for additional studies.

All of the mechanisms proposed above address the oxidation of biogenic amines. However, no mechanistic or computational studies have been performed on the irreversible acetylenic MAO inhibitors used in practice, such as rasagiline and selegiline (Figure 1). Knowledge of the mechanism of MAO inhibition is highly desirable for the design of new inhibitors, because the most widely used, rasagiline and selegiline, exhibit some adverse effects.[54,55] The disadvantages of selegiline treatment are mainly due to its amphetamine-like metabolites. Amphetamines further increase striatal dopamine levels, which is beneficial for relief of Par-

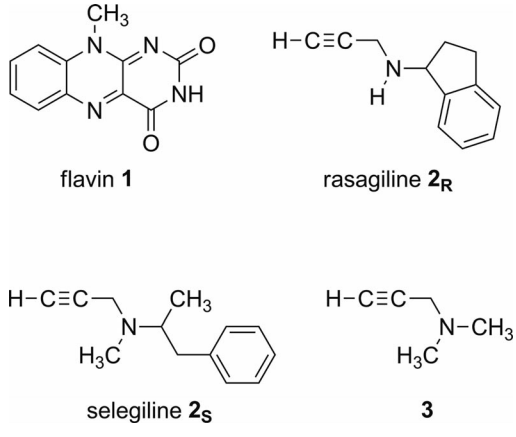

Figure 1. Structures of the flavin fragment and the irreversible acetylenic inhibitors investigated in this work.

kinson's disease symptoms, but can also cause psychological dependence. In addition to this, selegiline shows lower selectivity for MAO B than rasagiline and is capable of inhibiting MAO A in higher doses. This is beneficial for treatment of depression, a nonmotor symptom of Parkinson's disease, but on the other hand it results in hypertension, arrhythmias and hyperthermia. The use of rasagiline is accompanied by higher risks of liver function impairment and melanoma. The design and synthesis of new, safer and more efficient drugs are thus of significant importance, for which very detailed insight into the mechanism of inhibition is an essential requirement.

For these reasons we concentrated our computational study on the chemical binding of rasagiline and selegiline to the flavin moiety. The starting point of our study was the recently reported X-ray crystal structures of human MAO B irreversibly inhibited by rasagiline[56] or its analogues,[57] as well as with selegiline.[58] These structural determinations revealed that for both inhibitors a covalent bond between the flavin N5 nitrogen atom and the terminal acetylenic carbon atom is formed. In fact, to date, essentially all irreversible MAO inhibitors form N5 flavin adducts, although one notable exception is the flavin C(4a) adduct formed upon inhibition and ring opening with tranylcypromine.[59] Previous UV/Vis spectroscopy studies on small model systems by Maycock and co-workers[60] gave strong evidence that acetylenic inhibitors bind covalently to the enzyme in about one-to-one proportions. These findings were later unambiguously confirmed by detailed spectroscopic studies performed by Binda and co-workers.[61] On the basis of spectroscopic data, several researchers proposed that the formed adducts are highly conjugated.[23,60,62] Still, the precise natures of the reactions forming the complexes and structural details of bound inhibitors are as yet unknown, which leaves open the possibility of several inhibitor activation modes prior to reaction with the flavin. This is the crucial information for the development of new antidepressants and antiparkinsonian medications as more efficient MAO inhibitors and it represents the focus of the work presented here.

In order to determine in which form the inhibitor attacks the flavin moiety we propose a mechanism by which the adduct is formed as follows (Scheme 2). The underlying idea is that, prior to the chemical bond formation with the flavin, the inhibitor is firstly activated at the terminal carbon atom of the acetylene moiety or at the methylene site vicinal to the amino group. By activation we assume the abstraction variously of the hydride anion, the hydrogen atom or the hydrogen cation (proton) from either of these two carbon centres, performed either by the enzyme or by the polar environment. In total, this yields six possible mechanisms that need to be carefully studied (Scheme 2). In addition, we also took into account the approach of the neutral non-activated inhibitor, which is plausible and serves as a reference reaction.

The reason why we also considered the activation at the distant methylene centre is because any charge or radical density generated at this site could be transferred to the

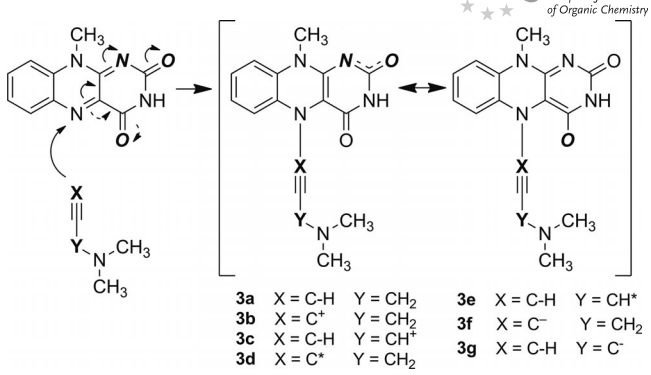

Scheme 2. Mechanisms of MAO B inhibition with selegiline and rasagiline. The final charge distributions on the denoted bold-italic nitrogen and oxygen atom depend on the forms of the inhibitors considered.

terminal acetylenic carbon atom, predominantly through resonance effects (Scheme 3), making the latter carbon spearhead prepared for the attack on flavin. It has to be said that the resonance stabilization depicted in Scheme 3 does not include resonance participation of the dimethylamino group or hyperconjugation effects, which all work towards the stabilization of such activated inhibitors. We propose that the rate-limiting step of the overall reaction is the formation of the covalent bond between the N5 atom of the flavin and the terminal carbon atom of the inhibitor to produce a covalent inhibitor–flavin adduct, in accordance with the X-ray spectroscopic data.[56–58] The formed adduct is further stabilized through resonance effects in flavin, as shown in Scheme 2.

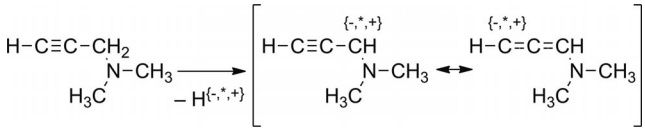

Scheme 3. Relevant resonance structures stabilizing the activated inhibitor produced by the abstraction variously of the hydride anion, the hydrogen atom or the proton at the methylene site.

Two alternative mechanisms of MAO B inhibition were proposed by Nakai and co-workers a decade ago.[63] These authors applied HF/6-31G(d) gas-phase calculations on a simplified pair of molecules – 3-formyl-2(1*H*)-iminopyrazine (**Ib**) and the propargylamine derivative **IIb** (Scheme 4) – as model compounds for the flavin moiety and the inhibitor, respectively. Both of their proposed mechanistic routes involve the formation of the two cyclic compounds **III** and **IV** as final products of the inhibition. Both reactions would take place, however, with kinetic barriers over 60 kcal mol^{-1}. In the same work,[63] these barriers were reduced to 50.3 and 46.9 kcal mol^{-1}, respectively, by employment of HF/3-21G methodology on the larger systems **Ia** and **IIa**. Still, in any of these ways, both sets of values are too high for enzymatic reactions to proceed at a significant rate, particularly in the context of the experimentally determined barrier heights for selegiline and rasagiline inhibition reactions – 21.3 and 20.8 kcal mol^{-1}, respectively[58,62] – used throughout this work. In addition, cyclic

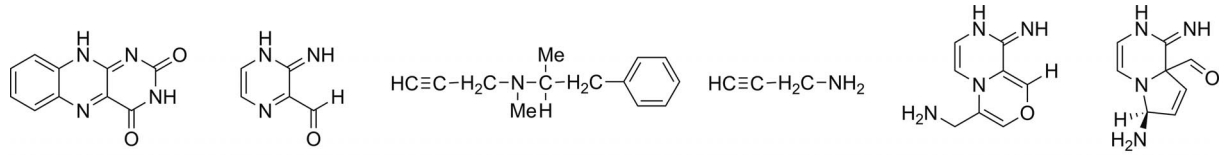

Scheme 4. Structures of the model systems **I** and **II** as reactants and the cyclic molecules **III** and **IV** as products of MAO B inhibition as proposed by Nakai et al.[63]

products of the inhibition are not supported by the X-ray structural analysis discussed above.[56–58] We therefore feel that the two mechanistic proposals by Nakai and coworkers play a minor role in the actual inhibition process.

The organization of this article is as follows: in Section 2 we describe the computational methods used, in Section 3 we discuss the results for the assumed mechanisms and in Section 4 we give conclusions and perspectives for future studies.

2. Computational Methodology

In order to calculate the free energy profile for the irreversible MAO B inhibition by rasagiline and selegiline we truncated the enzyme to the flavin moiety **1** and represented both inhibitors with the model system *N*,*N*-dimethylpropargylamine (**3**, Figure 1). All free energy profiles were obtained by starting from the optimized adduct and then artificially stretching the C(inhibitor)–N(flavin) chemical bond in relaxed 0.1 Å intervals. We assume that the inhibitor–flavin bond formation is the rate-limiting step of the overall reaction. In this study we did not consider the preceding inhibitor activation steps involving enzymatic H^+, $H^\cdot$ or H^- abstraction from the inhibitor.

As a good compromise between accuracy and practicality of the model, all molecular geometries were optimized by the very efficient B3LYP/6-31+G(d) method. Zero-point vibrational energies (ZPVEs) and thermal corrections were extracted from frequency calculations, obtained at the same level of theory, in which no scaling of the calculated harmonic vibrational frequencies was applied. All atomic charges were obtained at the same level of theory by employment of Natural Bond Orbital (NBO) analysis.[64] The final single-point energy calculations were achieved by use of a highly flexible 6-311++G(2d,2p) basis set with the B3LYP functional and the Boese–Martin for kinetics (BMK) method.[65] The first functional has frequently been shown in the literature to provide very accurate thermodynamic parameters for simple organic molecules, whereas the BMK approach has been particularly well parameterized and demonstrated to offer excellent accuracy for kinetic data. To account for the polarization effects caused by the rest of the enzyme, which are not explicitly included in our model, we performed single-point calculations with the conductor-like polarisable continuum model (CPCM),[66] as employed by Himo and coworkers.[67,68] This approximation assumes that the enzyme surroundings are a homogeneous polarisable medium with some conventionally defined dielectric constant. We performed calculations at the B3LYP/6-311++G(2d,2p) and BMK/6-311++G(2d,2p) levels of theory, employing the usual dielectric constant of $\varepsilon = 4$ and taking the rest of the parameters for pure water.[67] This gives rise to four computational models used here: namely B3LYP/6-311++G(2d,2p)//B3LYP/6-31+G(d) (denoted as **M1**), BMK/6-311++G(2d,2p)//B3LYP/6-31+G(d) (**M2**), (CPCM)/B3LYP/6-311++G(2d,2p)//B3LYP/6-31+G(d) (**M3**) and (CPCM)/BMK/6-311++G(2d,2p)//B3LYP/6-31+G(d) (**M4**). Open-shell species were treated with the unrestricted methodology. All thermodynamic parameters that correspond to the inhibition process are computed as reaction free energies. All calculations were performed with the Gaussian 09[69] suite of programs.

3. Results and Discussion

The Flavin Moiety and Inhibitors

Before we present the analysis of reaction mechanisms for MAO inhibition, let us first look at the Lewis/Brønsted acid–base properties of the isolated flavin fragment **1**, the inhibitor molecules $\mathbf{2_R}$ and $\mathbf{2_S}$ and the model system **3**. The purpose of this is twofold. Firstly, it should reveal some interesting inherent features of these compounds, which govern their reactivity in the enzyme active site, and secondly it should demonstrate and justify why the truncated system **3** is a very good model for representing the properties and reactivities of the two full-sized inhibitors rasagiline ($\mathbf{2_R}$) and selegiline ($\mathbf{2_S}$). In the process we consider the affinities of the flavin atoms N5 and O4 (Scheme 1) towards H^-, $H^\cdot$ and H^+ species, because these hydrogen systems are the smallest chemical models for larger molecular anions, radicals and cations, respectively. These values should serve as excellent probes of the reactivities of these two flavin sites, selected as available for the reaction with the incoming inhibitor/substrate in the enzyme. These affinities are calculated as the free energy changes of reactions (1) and (2).

$$\mathbf{1} + \mathbf{X} \rightarrow \mathbf{1X} \quad (1)$$

$$-\Delta G^\circ = \text{GB } (\mathbf{X} = H^+); \text{ HIA } (\mathbf{X} = H^-); \text{ HAA } (\mathbf{X} = H^\cdot) \quad (2)$$

GB, HIA and HAA represent the gas-phase basicity, the hydride ion affinity and the hydrogen atom affinity, respectively, when X corresponds to H^+, H^- and $H^\cdot$, respectively. Analogously, we also calculated the energies required to remove these three model species from the molecules $\mathbf{2_R}$, $\mathbf{2_S}$

and **3** to probe their intrinsic susceptibilities to activation for the inhibition reaction. Similarly to Equation (1), these are expressed as the changes in the free energy when the inhibitor molecules variously lose H^+, H^- or $H^\cdot$. All results are calculated in the gas phase and in dielectric media with use of the **M1** and **M3** models, respectively.

The results of this analysis are presented in Table 1. With regard to the flavin moiety **1** it turns out that the carbonyl oxygen is more basic than its imino nitrogen counterpart by 3.6 kcal mol^{-1} in the gas phase. This is not surprising because protonation at the oxygen atom yields the conjugate acid, which is more stabilized through cationic resonance than in the case of nitrogen protonation. This could easily be examined by inspecting the number of the cationic Lewis resonance structures. In addition, NBO population analysis reveals that in the neutral form the oxygen atom is more negative than nitrogen, with the assumption of atomic charges of –0.57 and –0.31 |e|, respectively. In addition, the carbonyl oxygen is more exposed to the inhibitor and the imino nitrogen is slightly more hindered. If these results were taken per se, they would predict that the cationic inhibitor would preferentially attack the oxygen site rather than the nitrogen atom, contrary to what was observed by X-ray analysis. However, inclusion of the medium-related effects reverses this picture. In solution, the imino nitrogen atom becomes more susceptible to the proton by 0.6 kcal mol^{-1}. We note in passing that solution values are less exergonic than the gas-phase results, because in the former case the reactant side in Equation (1) includes a very favourable contribution of the large solvation energy of the proton H^+. The same also holds for the corresponding HIA and, partially, the HAA values as presented below.

The situation with the hydride ion (HIAs) and the hydrogen atom affinities (HAAs) is less ambiguous than with proton affinities. In these two instances the flavin imino nitrogen is more favoured for the reaction in both phases, with the relative difference between two sites becoming even larger on moving to dielectric media. The condensed phase has very little influence on $H^\cdot$ addition reactions, because there is no major charge reorganization involved. Still, the **M3** model finds that the nitrogen N5 atom is over than 10 kcal mol^{-1} more inclined towards $H^\cdot$ attack than the carbonyl oxygen. These results therefore convincingly show that the flavin N5 imino nitrogen atom is the most favoured site for the inhibitor attack, which is consistent with numerous experiments performed on flavoenzymes.

The question of whether it is more advantageous to activate the inhibitor at the acetylene or the methylene carbon atom is even more interesting for MAO inhibition. Let us first consider deprotonation of the inhibitor to form the anion. In the gas phase it is slightly easier to remove the proton at the methylene site in both inhibitors $\mathbf{2_R}$ and $\mathbf{2_S}$. This is a consequence of the stronger anionic effect spread through the triple C≡C bond, which outstrips the strong acidity of acetylene protons because of a weak C–H bond strength due to the low *p*-content in the hybrid *sp* bonding orbital. In solution, in contrast, it becomes notably easier to strip off H^+ from the acetylene carbon atom. However, the difference of a few kcal mol^{-1} (or just a few pK_a units) is certainly not decisive in determining the mode of inhibitor activation through the anionic mechanism, but it could be a dominating effect. Interestingly, the two inhibitors $\mathbf{2_R}$ and $\mathbf{2_S}$, as well as the model system **3**, exhibit almost identical solution-phase acidities at the acetylene site, differing only by 0.2 kcal mol^{-1}, and very closely spaced methylene acidities (Table 1). Results for the hydride anion and the hydrogen atom abstractions strongly favour methylene activation, the difference in the former case being over 90 kcal mol^{-1} in both phases. This is not surprising, because upon H^- removal a cationic centre at the methylene site is formed and is stabilized by the strongly electron-donating ability of the vicinal dimethylamino group. The same also holds for the radical activation. This implies that, should the cationic and radical mechanism be operative in MAO, the corresponding activation of the inhibitor molecule would occur at the $–CH_2–$ group. Again, what cannot go unnoticed is the fact that both inhibitors exhibit very similar reactivities in these two cases, which we had also previously observed for the

Table 1. Gas-phase basicities (GBs), hydride ion affinities (HIAs) and hydrogen atom affinities (HAAs) of the selected flavin sites and free energies required to abstract the proton, the hydride anion and the hydrogen atom from the acetylene and methylene carbon atoms in inhibitor molecules as obtained with the computational models **M1** and **M3**.[a,b]

		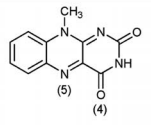 flavin **1**				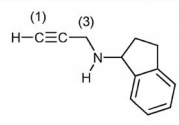 rasagiline $\mathbf{2_R}$		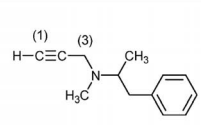 selegiline $\mathbf{2_S}$		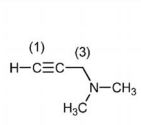 model inhibitor **3**	
atom		N5	O4	atom		C1	C3	C1	C3	C1	C3
GB (+ H^+)	M1	214.2	217.8	– H^+	M1	374.2	372.8	375.0	373.5	373.3	377.2
	M3	167.5	166.9		M3	252.8	256.4	252.6	257.3	252.8	258.3
HIA (+ H^-)	M1	91.4	71.3	– H^-	M1	282.2	190.2	275.8	185.7	284.9	191.2
	M3	60.8	38.5		M3	187.4	99.2	181.9	95.4	185.6	96.9
HAA (+ $H^\cdot$)	M1	58.3	50.2	– $H^\cdot$	M1	128.8	73.9	127.5	72.3	129.8	74.8
	M3	58.1	47.3		M3	125.0	73.4	121.8	72.1	125.2	74.4

[a] All values are in kcal mol^{-1}. [b] Computational levels of theory are denoted by **M1** and **M3**.

deprotonation. This is in agreement with the experimentally determined activation free energies for MAO inhibition by rasagiline and selegiline, which are almost identical with values of 20.8 and 21.3 kcal mol^{-1}, respectively.[62]

The last thing that should be commented upon is the fact that the truncated systems **3** provide excellent models for both inhibitors. It turns out (Table 1) that values for the molecule **3** very closely match the corresponding data for the full-sized inhibitors $\mathbf{2_R}$ and $\mathbf{2_S}$. This holds in particular for the most thermodynamically favourable sites for the inhibitor activation: namely the acetylene site for proton abstraction and the methylene carbon atom for the removal of H^- and $H^\cdot$. We can therefore reasonably conclude that molecule **3** can be used to model kinetic and thermodynamic features of rasagiline and selegiline in MAO inhibition.

In concluding this section it is worth summarizing that the simple analysis of the flavin Lewis/Brønsted acidity/basicity trends reveals that the nitrogen atom N5 is more favoured over the carbonyl oxygen for any form of inhibitor attack. Moreover, should the cationic or the radical inhibition mechanism be operative, the activation of the inhibitor should occur at the methylene site, whereas deprotonation of the inhibitor is more favoured at the terminal acetylene carbon. Still, because the difference in these two free energies of deprotonation is just a few kcal mol^{-1}, deprotonation is equally probable at both reactive carbon centres, particularly because one can imagine that specific interactions at the enzyme active site can easily change the corresponding pK_a values.

Inhibition Reaction

Results obtained for MAO inhibition reactions with the seven different forms of the model inhibitor **3a**–**3g** (Scheme 2) are presented in Table 2. These include activation ($\Delta G^{\#}_{act}$) and reaction free energies (ΔG_{react}) calculated

Table 2. Thermodynamic and kinetic parameters for the investigated modes of MAO inhibition as obtained with BMK/6-311++G(2d,2p)//B3LYP/6-31+G(d) (**M2**) and (CPCM)/BMK/6-311++G(2d,2p)//B3LYP/6-31+G(d) (**M4**) models. Selected inhibitor–flavin bond lengths and relevant imaginary frequencies are calculated with B3LYP/6-31+G(d) methodology.[a]

Inhibitor	$\Delta G^{\#}_{act}$[b]		ΔG_{react}[b]		d(N–C)$_R$[c]	d(N–C)$_{TS}$[c]	d(N–C)$_P$[c]	ν_{imag}[d]
	M2	M4	M2	M4				
H—C≡C–CH$_2$–N(CH$_3$)$_2$ **3a**	51.0	52.5	49.8	51.6	4.774	1.696	1.489	–372
⊕ C≡C–CH$_2$–N(CH$_3$)$_2$ **3b**	12.9	10.5	–51.2	–32.8	4.058	3.425	2.767	–48
	31.2	30.0	–62.1	–45.6	2.767	1.722	1.366	–495
H—C≡C–⊕CH–N(CH$_3$)$_2$ **3c**	20.2	26.7	8.8	21.1	4.084	1.928	1.526	–234
·C≡C–CH$_2$–N(CH$_3$)$_2$ **3d**	8.2	13.3	–50.0	–43.5	4.063	2.323	1.356	–89
HC≡C–·CH–N(CH$_3$)$_2$ **3e**	17.7	17.0	–4.8	–2.1	3.548	2.160	1.440	–285
⊖ C≡C–CH$_2$–N(CH$_3$)$_2$ **3f**	23.1	23.9	–40.8	–21.2	6.650	2.276	1.339	–155
H—C≡C–⊖CH–N(CH$_3$)$_2$ **3g**	3.4	5.9	–33.2	–19.8	6.468	3.741	3.169	–150
	28.3	29.0	–53.0	–37.9	3.169	3.881	1.394	–37
rasagiline $\mathbf{2_R}$	22.6 (20.8)$_{EXP}$[e]	19.9	–41.0	–26.9	6.660	2.266	1.338	–162
selegiline $\mathbf{2_S}$	25.7 (21.3)$_{EXP}$[e]	23.7	–38.8	–21.6	6.678	2.284	1.341	–154

[a] The inhibitors **3b** and **3g** react with flavin in two steps connected through two transition states. [b] Units: kcal mol^{-1}. [c] Units: Å; subscripts R, TS and P denote reactants, transition state and products, respectively. [d] Units: cm^{-1}. [e] Experimental data are taken from ref.[58,62].

in the gas (**M2**) and condensed phases (**M4**), relevant C(acetylene)–N5(flavin) distances, and values of imaginary frequencies in the transition state (ν_{imag}) corresponding to the molecular vibrations connecting reactants with products. Geometric parameters and charge distributions in different forms of inhibitors are given in Table 3.

Table 3. Selected geometrical parameters (d, in Å) and NBO-based atomic charge distributions (q, in |e|) in the isolated inhibitors (in round brackets) and after binding to the flavin (in square brackets) obtained with B3LYP/6-31+G(d) model. Total charge on the inhibitor molecule is given with q_{INH}.

(1) (2)(3) (4)
H—C≡C-CH_2-NMe_2

Inhibitor	d_{C1-C2}	d_{C2-C3}	d_{C3-N4}	q_{C1}	q_{C2}	q_{C3}	q_{N4}	q_{INH}
(3a)	1.211	1.480	1.464	–0.25	–0.05	–0.33	–0.54	0.00
[3a]	1.316	1.438	1.432	–0.12	0.04	–0.32	–0.51	0.29
(3b)	1.314	1.466	1.495	0.39	–0.27	–0.18	–0.28	1.00
[3b]	1.212	1.463	1.461	0.13	0.17	–0.35	–0.54	0.42
(3c)	1.213	1.404	1.301	0.03	–0.17	0.17	–0.28	1.00
[3c]	1.295	1.340	1.352	–0.12	–0.11	0.03	–0.44	–0.23
(3d)	1.257	1.474	1.464	0.01	–0.29	–0.32	–0.40	0.00
[3d]	1.211	1.465	1.466	0.13	0.06	–0.33	–0.54	0.23
(3e)	1.229	1.383	1.387	–0.25	–0.12	–0.11	–0.45	0.00
[3e]	1.315	1.322	1.389	–0.07	–0.11	–0.04	–0.50	0.28
(3f)	1.250	1.472	1.498	–0.40	–0.49	–0.32	–0.57	–1.00
[3f]	1.217	1.458	1.479	0.20	–0.10	–0.32	–0.55	0.06
(3g)	1.287	1.354	1.463	–0.62	–0.12	–0.36	–0.57	–1.00
[3g]	1.327	1.317	1.420	–0.03	–0.16	–0.09	–0.53	0.07

The first thing evident from the data in Table 2 is the fact that inclusion of CPCM environment polarization effects introduces certain changes into values of thermodynamic data, but the general picture remains the same. The largest environmental influence is on the reaction free energies, which as a rule become more positive or less exergonic after CPCM correction. This influence is lowest in uncharged systems: namely in the neutral **3a** and the radicals **3e** and **3d**, where it is 1.8, 2.7 and 6.5 kcal mol^{-1}, respectively. It increases in charged systems, culminating in **3f**, where it alters the gas-phase value by 19.6 kcal mol^{-1}.

The impact of dielectric medium on the activation free energies is much smaller, ranging from 0.7–6.5 kcal mol^{-1}. In a majority of cases $\Delta G^{\#}_{act}$ values slightly increase after CPCM correction, but there are few notable exceptions. In the rest of the text, when discussing kinetic and thermodynamic aspects of the inhibition reactions we use data obtained with CPCM methodology representing the enzyme environment (model **M4**). It is also worth noting that the inhibitors **3a** and **3c**–**3f** bind to the flavin in one-step processes involving single transition structures, whereas inhibitors **3b** and **3g** each react in two steps connected with two transition states.

We start our analysis with the neutral non-activated inhibitor **3a**. It can attack the flavin N5 atom through a favourable interaction between the flavin LUMO and the inhibitor HOMO of the triple bond. The fact that the flavin acts as an electrophile is evident from the data in Table 3. Upon binding, the inhibitor molecule loses some electron density to the flavin as the total NBO atomic charge on the former is 0.29 |e|. The charge on the terminal carbon atom is reduced in half by 0.13 |e| and the triple C1≡C2 bond becomes elongated from 1.211 to 1.316 Å. This excess positive charge is spread over the rest of the inhibitor molecule as both C2–C3 and C3–N4 bonds become slightly shortened. As the inhibitor approaches, at the C(inhibitor)–N5(flavin) distance of 4.774 Å a reactive complex almost 10 kcal mol^{-1} less stable than the separated reactants is formed (Figure 2). The transition state in this reaction is very late, with the C–N5 distance reduced to 1.696 Å, being 1.489 Å in the final covalent adduct. The free energy of activation for this reaction is very large, at 52.5 kcal mol^{-1}. What is even more unfavourable is that the overall reaction is largely endergonic, ΔG_{react} having the highly positive value of 51.6 kcal mol^{-1}. This means that the formed adduct is not very long-lasting, because it is much less stable than the sum of the reactants on the free energy ladder, which taken all together gives strong evidence that the inhibition reaction is very unlikely to proceed by this mechanism. However, we did locate two more stable products formed upon addition of **3a** to the flavin **1**: namely the tetracyclic **3a**–**c1** and the exacyclic **3a**–**c2** (Scheme 5), which are lower in energy by 32.9 and 48.7 kcal mol^{-1}, respectively (Figure 2). The two compounds are analogous to the already mentioned molecules **III** and **IV** of Nakai and co-workers (Scheme 4),[63] who showed that both cyclization reactions

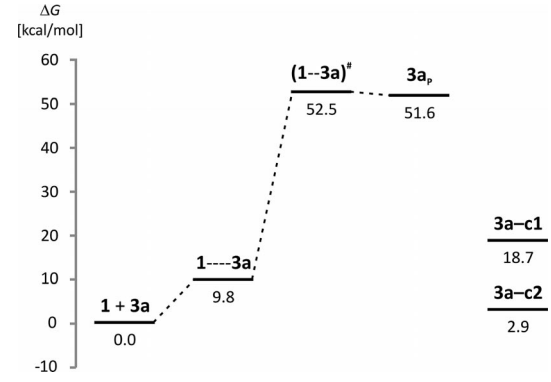

Figure 2. Reaction profile for the binding of the neutral inhibitor **3a** to the flavin **1** to yield the acyclic product $\mathbf{3a_P}$. Energies of other two cyclic product alternatives **3a**–**c1** and **3a**–**c2** are also given. All values are in kcal mol^{-1} and were obtained with the **M4** model.

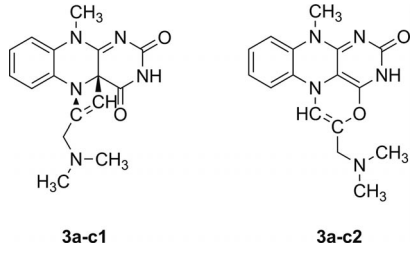

Scheme 5. Two possible cyclic products formed upon the addition of the neutral inhibitor to the flavin moiety.

are associated with very large barriers (over 60 kcal mol^{-1}) to be crossed in enzymatic reactions. Because of this, and because X-ray analysis had revealed acyclic inhibition products, we did not consider any mechanistic aspects involving these two cyclic compounds. Moreover, although significantly more stable than **3a**$_{\mathbf{P}}$, both of the cyclic adducts **3a**–**c1** and **3a**–**c2** are less stable than the sums of their building blocks (Figure 2), implying that both reactions leading to these products are endergonic. We can therefore reasonably conclude that attack on the flavin by the non-activated neutral inhibitor is in any event very unlikely to happen.

Let us now switch our attention to two cationic mechanisms, in which the inhibitor is activated by removal of hydride anion (H^-) from the terminal acetylene carbon atom in **3b** and from the methylene group in **3c**. We have already reported that it is around 90 kcal mol^{-1} easier to strip H^- from the methylene centre (Table 1), but the complete thermodynamic picture of the inhibition reaction is not more favourable for **3c**. Abstraction of the hydride anion from the methylene site produces a planar **3c** cation, which is very stable per se due to favourable interaction with the strongly electron-donating vicinal dimethylamino group. As will become clear later, such resonance stabilization is almost completely absent in the related **3b** cation. To estimate the strength of this interaction we performed calculations in which we rotated the $-NMe_2$ group in **3c** around the C–N bond, while keeping the rest of the geometry frozen. The electronic energy of this artificial system increased to a maximum of 69.2 kcal mol^{-1} [B3LYP/6-31+G(d) model], corresponding to a dihedral rotation of approximately 90°, giving a rough estimate of the magnitude of the resonance stabilization. Interestingly, this very simple consideration gives a value that matches very well the energy difference mentioned above required to abstract H^- from both carbon sites in **3b** and **3c**, which can therefore almost exclusively be attributed to the resonance effect in both cations. The resonance stabilization in **3c** is further in evidence because the C3–N4 bond length is greatly reduced from 1.464 Å in **3a** to 1.301 Å in **3c**. Interestingly, the length of the triple C≡C bond in **3c** remains unchanged before and after H^- removal. Therefore, upon formation of a cation, an excess positive charge remains close to the methylene centre in **3c**. The atomic charge on this carbon atom is increased by as much as 0.50 |e| after H^- abstraction (Table 3). This leaves the attacking acetylene carbon atom with no charge [$q(C1)_{3c}$ = 0.03 |e|] to act as a nucleophile in the inhibition. Moreover, after the binding the total atomic charge on the inhibitor molecule **3c** is increased from 1.00 to –0.23 |e|, implying that **3c** took one and a quarter electrons from the flavin to produce covalent bonding. As will be shown later, this is an unfavourable situation, because flavin is a pronounced electrophile, so the overall binding of **3c** to the flavin **1** is an endergonic process and thus unlikely to occur.

To come close to the flavin, it costs 4.8 kcal mol^{-1} for **3c** to form the reactive complex and an additional 21.9 kcal mol^{-1} to arrive at the transition state, so the total activation energy for this mechanism equals 26.7 kcal mol^{-1}. After this, **3c** binds to the flavin, stabilizing the transition state structure by just 5.6 kcal mol^{-1} and restoring much of its initial electron distribution in the acetylenic region (Table 3). The resulting flavin adduct is not very stable and the corresponding reaction free energy is highly positive [ΔG_{react}(**3c**) = 21.1 kcal mol^{-1}]. Although the barrier height is reasonable and in fair agreement with experimental results the overall endergonic character of this process makes it unlikely to take place. As such, we can conclude that the activation of the inhibitor through the abstraction of the H^- anion at the methylene carbon does not play a significant role in MAO inhibition.

On the other hand, cation **3b** produced at the acetylene site is even more electrophilic than **3c**, yet not particularly intrinsically stabilized. Upon H^- removal, significant geometric change is imposed only on the triple C–C bond, which is elongated by 0.1 Å. The cation **3b** will therefore be more likely than **3c** to try to bind the flavin to one of its reactive sites to gain some stabilization afterwards. Interestingly, when approaching the flavin fragment, the cation **3b** first binds to the carbonyl oxygen atom O4 in a *trans* orientation with the respect to the flavin N5 atom, without any kinetic barrier (Figure 3). The process is favourable and the reaction free energy is ΔG_{react} = –37.2 kcal mol^{-1} at the **M4** level of theory. To position itself for the reaction with the flavin N5 atom the inhibitor must then rotate around the carbonyl C=O bond to arrive at the *cis* oxygen adduct, which is 4.4 kcal mol^{-1} less stable than the *trans* complex. This process is associated with a barrier height of 10.5 kcal mol^{-1}. Because the flavin nitrogen N5 atom is more reactive towards cationic inhibitors than carbonyl oxygen (Table 1), the adduct of **3b** with the N5 atom is even more stable than the two oxygen *trans* and *cis* complexes, by an additional 8.4 and 12.8 kcal mol^{-1}, respectively (Figure 3). To move from the flavin oxygen to the nitrogen atom, the cation **3b** must surmount a kinetic barrier of 30.0 kcal mol^{-1}. This represents the rate-limiting step of the whole process. During it, the C(inhibitor)–O4(flavin) bond length changes from 1.331 Å (reactants) through 1.442 Å

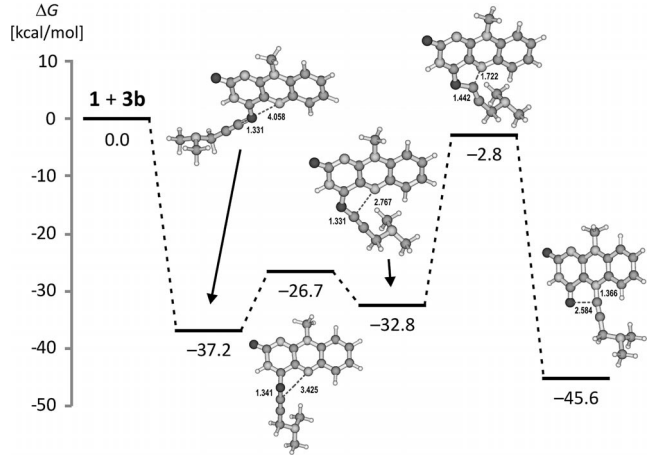

Figure 3. Reaction profile for the reaction between the flavin **1** and the cation **3b** obtained at the (CPCM)/BMK/6-311++G(2d,2p)//B3LYP/6-31+G(d) level of theory. All values are in kcal mol^{-1}.

(transition state) to 2.584 Å (products), while the corresponding C(inhibitor)–N5(flavin) bond decreases in the same manner, taking values of 2.767, 1.722 and 1.366 Å. It is interesting to note that the carbon–oxygen bond length in the first complex and the carbon–nitrogen bond length in the final product are practically identical, being only slightly larger in the latter case. This is qualitative evidence that the nitrogen atom, despite being sterically much more hindered than oxygen, is more reactive than oxygen towards cationic inhibitors, because the inhibitor can approach it equally close as it can the oxygen atom. This is consistent with the already observed intrinsic reactivities of these two flavin sites (Table 1). The process of MAO inhibition by the activated compound **3b** is thermodynamically feasible and could occur. The overall reaction is exergonic (ΔG_{react} = –45.6 kcal mol^{-1}), but the total activation free energy for this process – $\Delta G^{\#}_{act}$(**3b**) = 34.4 kcal mol^{-1} – is much higher than the experimentally determined values for rasagiline and selegiline, of 20.8 and 21.3 kcal mol^{-1}, respectively. This reduces the probability that the true inhibition reaction proceeds through this mechanism. As will become apparent later, there is another inhibition mechanism with overall exergonic character, but with a barrier height much closer to those observed experimentally.

Now we will consider radical mechanisms involving the activated inhibitors **3d** and **3e**. Just like with cationic inhibitors **3b** and **3c**, it turns out that the results for isolated molecules suggest that the **3e** tautomer should be more reactive, because it is around 50 kcal mol^{-1} easier to produce the radical at the methylene carbon centre than at the terminal acetylene site. The reason is again the same: favourable participation of the vicinal electron-donating dimethylamino group in **3e**. To allow some quantitative measure of this effect, we repeated the calculation presented for the cationic inhibitor **3c** involving artificial rotation of the –NMe_2 group around the C–N bond in **3e**. As expected, the resonance effect is not so large in **3e**, with a value of 14.2 kcal mol^{-1}. Still, it is further evidenced in the electronic redistribution upon H$^{\cdot}$ detachment, in which the relevant C3–N4 and C3–C2 bonds are shortened from 1.464 and 1.480 Å to 1.387 and 1.383 Å, respectively (Table 3). This is reflected in the change in atomic charges in **3e**, in which the radical centre C3 atom loses 0.22 |e| of its previous electron density due to the H$^{\cdot}$ removal. Surprisingly, the charge on the terminal C atom remains the same. Quite interestingly, when the radical **3d** is formed, there is practically no change in the geometry of the inhibitor. All three relevant chemical bonds remain almost the same (Table 3), which can also be said, to a good approximation, for the atomic charges (there is just some charge redistribution between C1–C2). This is evidence that the radical **3d** is unstable. It is not stabilized intramolecularly through resonance effects, because its singly occupied molecular orbital (SOMO) is the *sp*-hybrid orbital, which is colinear with the atoms C1–C3 and perpendicular to the π electron system of the triple bond. Therefore, analogously to the **3b**–**3c** pair, the radical **3d** should react more readily with the flavin because of its intrinsic lower stability (Figure 4).

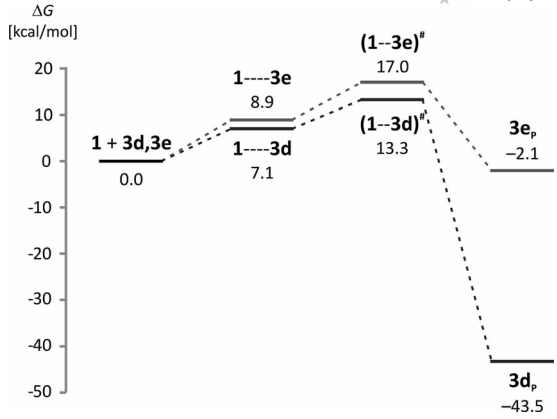

Figure 4. Reaction profile for the reaction between the radical inhibitors **3d** and **3e** and the flavin **1** obtained at the (CPCM)/BMK/6-311++G(2d,2p)//B3LYP/6-31+G(d) level of theory. All values are in kcal mol^{-1}.

The data in Table 2 and the graphical representation in Figure 4 indeed reveal that the radical **3e** is less reactive than **3d** towards the flavin. When the two radical inhibitors are approaching the flavin, the corresponding reactive complexes see **3e** closer to the flavin than **3d**. The related C(inhibitor)–N(flavin) bond lengths are 3.548 and 4.063 Å, respectively. This is why is takes a little more energy for the flavin **1** to form a reactive complex with **3e** (ΔG = 8.9 kcal mol^{-1}) than with **3d** (ΔG = 7.1 kcal mol^{-1}). The difference in carbon–nitrogen bond lengths is further reduced in the transition state structures, being 2.160 and 2.323 Å for **3e** and **3d**, respectively. Interestingly, these differences are completely reversed in the formed adducts. The inhibitor **3d** binds more strongly to flavin, with the corresponding C–N distance of 1.356 Å, relative to the 1.440 Å found in **3e**. After **3e** has bound to the flavin, the terminal C1–C2 bond is further elongated. The charge on the C1 atom decreases by 0.18 |e| and the total charge on the inhibitor becomes 0.28 |e|, giving strong evidence that **3e** acts as a nucleophile in the complexation reaction, which is favourable. The same change in the atomic electron densities is also observed for the radical inhibitor **3d**, in which case the charge on the terminal carbon atom changes from 0.01 to 0.13 |e| upon binding and the inhibitor loses 0.23 |e| of its electron density.

Interestingly, when **3d** reacts with the flavin, it completely restores its geometry from the isolated neutral molecule **3a**, by reducing the triple C1–C2 bond to 1.211 Å, identical to the case in **3a**. In other words, the geometry change in **3a** imposed by the abstraction of H$^{\cdot}$ to form **3d** is completely reestablished upon binding to flavin. During the whole process the inner chemical bonds C2–C3 and C3–N4 in **3d** also change within only small ranges of 0.015 and 0.002 Å, respectively. This is additional evidence that the radical formation in **3d** and the binding to the flavin are local events for this inhibitor.

The radical inhibitor **3e** reacts very gently with flavin, because of its intrinsic high stability. The free energy of activation for **3e** is $\Delta G^{\#}_{act}$ = 17.0 kcal mol^{-1}, a bit higher than

in **3d**. The overall reaction is exergonic, but only slightly, with $\Delta_r G$ = –2.1 kcal mol^{-1}. Although the kinetic barrier to this reaction is very low, the change in the reaction free energy is negligible, which suggests that the whole inhibition process would be in the equilibrium. This means that the reverse reaction, in which the formed adduct would decompose into its constituting fragments **3e** and **1**, would be equally probable as the complex-forming reaction. This is certainly not the case in the MAO B enzyme, however, because both rasagiline (**2$_R$**) and selegiline (**2$_S$**) are irreversible inhibitors, meaning that once they covalently bind to flavin very stable adducts are formed. An inhibition reaction with the activated methylene-centred radical **3e** could therefore be ruled out as the predominant mechanism of MAO B inhibition.

The radical **3d** exhibits a very favourable kinetic and thermodynamic picture of the inhibition. The kinetic barrier is still lower, being just $\Delta G^{\#}_{act}$(**3d**) = 13.3 kcal mol^{-1}, and the process of binding is very beneficial, with ΔG_{react} = –43.5 kcal mol^{-1}. Of all the mechanisms investigated here, the inhibition reaction involving molecule **3d** displays the lowest kinetic barrier and second (to **3b**) most favourable exergonic character of the overall reaction. These results suggest that the inhibition reaction would proceed through this mechanism. However, there are several reasons why we do not favour radical involvement in MAO B inhibition reactions. First of all, as already mentioned in the Introduction, several experiments that failed to supply evidence for radicals or radical intermediates during MAO activity have been performed. The only exception was provided by recent spectroscopic studies by Rigby et al.,[70] which suggested the presence of a tyrosyl radical in partially reduced human MAO A enzyme. This idea was later abandoned, though,[71] due to improper techniques used in the previous work.[70] In addition, the already mentioned Hammett correlation of MAO activity for a set of *para*-substituted benzylamines[36] gives strong evidence for the polar mechanism over the radical mechanism. Silverman defended his radical mechanistic proposal by arguing that "if radical intermediates are formed, they must be very short lived, low in concentration, or spin paired with another radical".[39] This could be true for the catalytic activity of a MAO enzyme, because to perform its role of converting amines to imines, the enzyme needs to abstract two hydrogen atoms from the substrate, a two-step process, which could in the radical context turn out to be too fast or too coupled to be experimentally detectable. In the proposed radical inhibition reaction, however, only one hydrogen atom should be abstracted to activate the inhibitor. Afterwards, the newly generated compound would attack the flavin moiety to form a very stable covalent radical adduct. This would allow enough time for unpaired radical spin density to be detected experimentally, so it is very likely that the MAO inhibition reaction does not involve radical species, although the catalytic activity of this enzyme could perhaps still proceed through a radical mechanism. It is important to emphasize that our results do not rule out the possibility of a radical mechanism in a catalytic step, because there are numerous literature examples of enzymes in which catalytic activity and inhibition are the results of different mechanisms. A second reason ruling out a radical inhibition mechanism is that all X-ray analyses and subsequent mechanistic and structural studies performed on MAO enzymes have established that in this family of enzymes there are no classical radical initiators to start the radical reaction. Enzymatic radical reactions are initially initiated by radical generating systems, exemplified by various coenzyme B12-dependent enzymes[72,73] or by ribonucleotide reductase.[74–76] Thirdly, we have already demonstrated that the acetylene-centred radical **3d** is not very stable, because it affords no intramolecular stabilization of the radical centre. This is not surprising because it is well documented in the literature that radicals with triple bonds are intrinsically of low stability.[77–91] As such, their generation is an unfavourable process. Finally, in a very recent study Erdem and Büyükmenekşe[92] proposed a biradical mechanism for MAO catalysis, but in the same paper the authors declared it improbable, on the basis of the obtained inverse Hammett correlation between the calculated log(k) values and the substituent σ-constants for a set of nine *para*-substituted benzylamine substrates and a subsequent poor correlation (R = 0.78) between the calculated and experimentally determined log(k) values. The authors concluded that these results "present negative evidence for the modelled biradical mechanism".[92] In finishing this section, we can say, from the results and arguments presented, that radical mechanisms of inhibition are not operative in MAO enzymes. Still, the results offered are useful for comparative purposes and for the completeness of the study.

We finally focus on two anionic mechanisms, which involve inhibitors activated by proton detachment from acetylene (**3f**) and methylene carbons (**3g**). We have already demonstrated that their solution free energies of deprotonation differ only by 5.5 kcal mol^{-1} in favour of the acetylene carbon (Table 1). This difference is too small for clear distinction between two inhibitor forms. We have also showed that it is important for a successful inhibitor to have a lot of negative charge on the acetylenic spearhead to act as a nucleophile during inhibition. By that argument, the methylene activated system **3g** should be a less potent inhibitor than its **3f** counterpart.

In the deprotonated form **3g** carries –0.62 |e| atomic charge on the terminal carbon atom. This is reduced to only –0.03 |e| upon binding, which reveals the electrophilic character of the flavin. In the product the charge on the inhibitor molecule is 0.07 |e|, which means that the flavin molecule accommodates almost a whole electron from the inhibitor. Analogously to **3b**, the reaction with **3g** proceeds in two steps (Figure 5). In the approach of **3g** to the flavin, at a C1(inhibitor)–N5(flavin) distance of 6.468 Å a reactive complex is formed. After that, there is a barrier of just 1.0 kcal mol^{-1} to arrive at the intermediate, which is almost 20 kcal mol^{-1} more stable than the non-interacting fragments. This complex is characterized by a small terminal C(inhibitor)–C(9a) bonding distance of 1.560 Å. This is not surprising, because in the neutral form the flavin carbon atom C(9a) is significantly positive, with a NBO charge of

0.19 |e|. The final product of the inhibition is 18.1 kcal mol^{-1} more stable than the intermediate. To proceed to the former, **3g** needs to cross a barrier of 29.0 kcal mol^{-1}. Although the overall exergonicity of this reaction is very favourable (ΔG_{react} = –37.9 kcal mol^{-1}), the calculated barrier is too much higher than experimentally determined values to give preference to this mechanism.

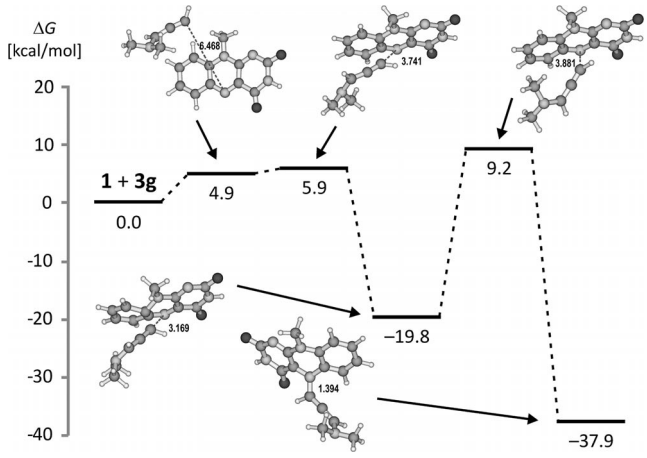

Figure 5. Reaction profile for **3g** anion obtained with the (CPCM)/BMK/6-311++G(2d,2p)//B3LYP/6-31+G(d) model. All values are in kcal mol^{-1}.

With the activated inhibitor **3f**, on the other hand, the inhibition reaction is carried out in one step (Figure 6). The overall reaction is exergonic by ΔG_{react}(**3f**) = –21.2 kcal mol^{-1}. The formed complex is characterized by a bonding flavin–inhibitor distance of 1.339 Å. Interestingly, this is the shortest carbon–nitrogen bond in all adducts investigated here. Before the attack, the terminal carbon atom carries –0.40 |e| of negative charge, and almost 90% of the inhibitor excess negative charge is shared between this and its neighbouring acetylenic carbon atom, which is very beneficial for the inhibition reaction. NBO analysis shows that, after binding, the charges on this carbon atom and on the whole inhibitor molecule are reduced by 0.60 |e| to 0.20 |e|

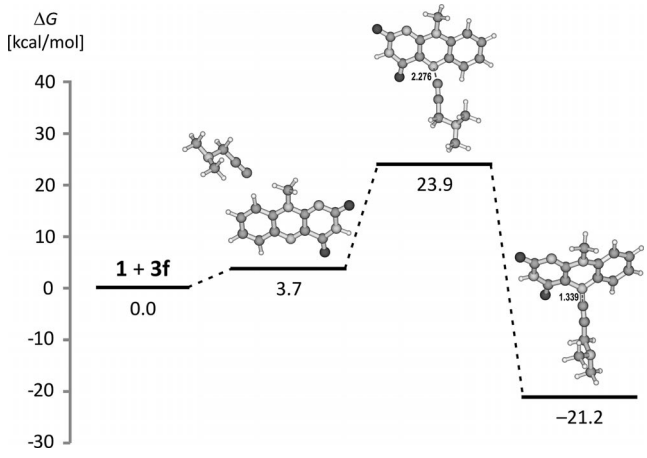

Figure 6. Reaction profile for the anion **3f** obtained with the (CPCM)/BMK/6-311++G(2d,2p)//B3LYP/6-31+G(d) model. All values are in kcal mol^{-1}.

and by 0.94 |e| to 0.06 |e|, respectively. This again shows that the flavin molecule behaves as an electrophile in the inhibition process and that it is very ready to accommodate negative charge. The kinetic barrier connecting reactants and the product is 23.9 kcal mol^{-1} at the **M4** level of theory, thus being in very good agreement with the experimentally determined values for rasagiline and selegiline of 20.8 and 21.3 kcal mol^{-1}, respectively (Table 2).

These results suggest that the MAO inhibition process occurs through a polar anionic mechanism involving the inhibitor molecule **3f**, being activated by deprotonation at the terminal acetylene site prior to binding to the flavin **1**. This result is consistent with experiments performed by Miller and Edmondson,[36] who showed that attaching electron-withdrawing groups to the *para*-position of the benzylamine substrate increases the rate of the reaction in MAO A, which gives strong support to a polar mechanism. The same argument was used by Erdem and Büyükmenekşe[92] to rule out a biradical catalytic mechanism of MAO enzymes. Additional evidence in favour of the anionic polar mechanism is the geometry of the flavin subunit in the formed adduct. Edmondson and coworkers[22] demonstrated that in the inhibition product the flavin structure is bent by ca. 30° from planarity around the axis connecting the N5 and N10 atoms. If we consider the dihedral angle involving the flavin atoms C(9a)–N(10)–N(5)–C(4a) it assumes 27.6° for **3f**, which is in excellent agreement with the described experimental result.[22] These data are also well matched in **3g**, where the angle is 29.8°. In other cases the formed adducts exhibit more planar conformations of the flavin fragment, with dihedral angles of 8.2, 0.2, 5.5, 10.9 and 10.3° for **3a**–**3e**, respectively.

The results presented here offer useful guidance for the design and preparation of new antidepressants and antiparkinsonian drugs as MAO inhibitors. We have clearly demonstrated that in any mechanism considered, but in the most feasible involving inhibitor **3f** in particular, the flavin moiety acts as an electrophile and efficiently accommodates negative charge from the inhibitor. We believe that this represents crucial information for both the inhibition and the catalytic activity of MAO enzymes. Therefore, promotion of nucleophilicity of the potential MAO inhibitor, while maintaining the energy cost to activate it by the enzyme as low as possible, is a promising strategy for more efficient compounds.

Rasagiline and Selegiline

Rasagiline ($\mathbf{2_R}$) and selegiline ($\mathbf{2_S}$) are in practical use as acetylenic MAO B inhibitors for treatment of symptoms of Parkinson disease. After having established the most likely inhibition mechanism with model systems, we decided to apply it to the full-sized inhibitors $\mathbf{2_R}$ and $\mathbf{2_S}$, for which experimentally determined free energies of activation are known.[58,62] This should serve as further validation for the proposed anionic mechanism. We again modelled chemical bond formation between the inhibitor terminal carbon

atom and the flavin N5 atom in accordance with the determined X-ray structures.[56–58] Results are presented in Table 2, whereas the structure of the reactants, products and transition states for both inhibitors are depicted in Figure 7.

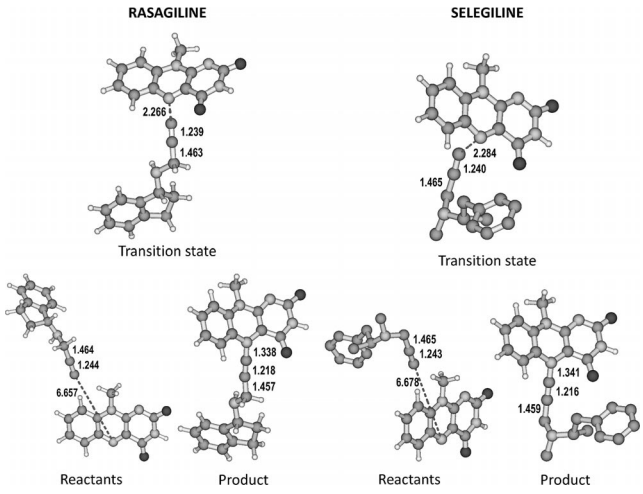

Figure 7. Structures of reactants, transition states and products for rasagiline ($\mathbf{2_R}$, left) and selegiline ($\mathbf{2_S}$, right) reacting with flavin. Hydrogen atoms on the selegiline were omitted for reasons of clarity.

It turned out that all thermodynamic and geometric data for both inhibitors $\mathbf{2_R}$ and $\mathbf{2_S}$ follow what was established for the model system **3f**. In all three cases the overall chemical reactions are exergonic, ranging from –21.2 kcal mol^{-1} found for **3f** to –21.6 and –26.9 kcal mol^{-1} calculated for $\mathbf{2_S}$ and $\mathbf{2_R}$, respectively. Geometrical data for all three compounds are also very similar for all stationary points along the reaction. Rasagiline and selegiline exhibit somewhat lower free energies of activation than the model system **3f**, at 19.9 and 23.7 kcal mol^{-1}, respectively, in very good agreement with the experimentally determined values of 20.8 and 21.3 kcal mol^{-1}, respectively. The geometries of the flavin subunits in the formed products are again bent, as calculated for the model system **3f**. The dihedral angles encompassing the flavin atoms C(9a)–N(10)–N(5)–C(4a) are 27.1 and 27.4° for $\mathbf{2_R}$ and $\mathbf{2_S}$, respectively, which is consistent with the experimental observations of Edmondson and co-workers[22] mentioned above.

As observed, there is a slight but notable difference of 0.5 kcal mol^{-1} in the experimentally measured activation free energies for rasagiline ($\mathbf{2_R}$) and selegiline ($\mathbf{2_S}$). In terms of the rate constants, this would imply that $\mathbf{2_R}$ should react with the flavin two to three times more rapidly than $\mathbf{2_S}$. This suggests that during MAO inhibition a major role is played by the identical propargylamine components in both inhibitors, but that the function of the rest of the inhibitor molecule is also significant. Interestingly, the calculated activation free energies for $\mathbf{2_R}$ and $\mathbf{2_S}$ are lower than for the truncated inhibitor **3f**, in which the aromatic part of the molecule is missing. It seems that these aromatic fragments are used by the enzyme to promote the binding of the inhibitor, most likely through π–π and σ–π noncovalent interactions.

Both of the calculated activation free energies and their very good agreement with the available experimental data, the overall exergonic character of the reaction and the flavin geometries in the end products lend credence to the considered acetylenic anionic mechanism of MAO–B inhibition. This information could be useful for the design of new compounds against Parkinson's disease.

4. Conclusions

In this manuscript we have computationally investigated the inhibition of the enzyme monoamine oxidase B (MAO B) by the irreversible inhibitors rasagiline and selegiline, which are both in practical use for relief of symptoms of Parkinson disease. To elucidate the mechanism of the reaction we truncated the enzyme to the flavin subunit and represented both inhibitors with the model system *N*,*N*-dimethylpropargylamine. This turned out to be legitimate after a careful analysis of the intrinsic Brønsted/Lewis acid/base properties of two reactive sites on the model system relative to the full-sized inhibitors. The starting points of our study were X-ray structures that revealed covalent bonding between the inhibitors' terminal carbon atoms and the flavin N5 atom. We assumed that the formation of these bonds is the rate-limiting step of the inhibition process and considered seven forms of the inhibitor yielding seven different mechanisms. These include the neutral inhibitor and six enzymatically initiated systems, formed by H^+, H^- and $H^\cdot$ abstraction from the terminal acetylene or the distal methylene groups prior to reaction with the flavin. We showed that in favourable reactions the flavin reacts as an electrophile, accommodating excess negative charge from the inhibitor upon binding.

The calculated reaction profiles were sufficient to differentiate between different reaction pathways and to rule out or substantiate suggested mechanisms. In terms of the overall exergonic character of the reaction, with comparison between calculated and experimentally determined free energies of activation, we demonstrated that the polar anionic mechanism involving inhibitor deprotonated at the acetylene carbon atom is the most plausible. This mechanism was additionally validated by inspection of the geometries of the flavin moieties in the formed adducts, which exhibit distortion from planarity consistent with experimental observations.[22] Calculations on the full-sized inhibitors rasagiline and selegiline with the same mechanism yielded free energies of activation of 19.9 and 23.7 kcal mol^{-1}, respectively, which are in a very good agreement with experimentally determined values of 20.8 and 21.3 kcal mol^{-1}, respectively.

The results of this study could be of significant importance for the pharmaceutical industry in terms of the design and the synthesis of new antiparkinsonian drugs. This is important, because both rasagiline and selegiline, although in wide practical use, display several adverse effects. Estimated revenue of MAO B inhibitors used as antiparkinso-

nians exceeded four billion dollars in 2009. From the results presented in this study, we feel that a useful strategy for the development of new compounds would be to promote nucleophilicity of the activated inhibitor, while keeping the energy required for its deprotonation as low as possible. In addition, inhibitors' selectivities for MAO A or MAO B isoforms should be enhanced. To achieve this purpose one should proceed with QM/MM studies of these reactants with suitable thermal averaging and appropriate free energy calculations.[50] This should be performed in order to model the reaction more accurately by taking into account the entire enzyme and the surrounding solvent.[93,94] In this work we did not consider the initial step of enzymatic inhibitor deprotonation, although it is reasonable to assume that it does not represent the overall rate-limiting step. It should be facile, because both the enzyme and the cytoplasm are proton-rich environments. Still, locating the enzyme proton acceptor for the incipient step of MAO inhibition remains a challenge for future studies. This is a difficult task, because a simple consideration of pK_a values of appropriate ionisable groups is not sufficient. Studies of pK_a values of enzyme active centres are associated with large experimental difficulties, whereas computational treatment is often unreliable; it was recently demonstrated, for example, that ionisation of Glu66 in the hydrophobic site of staphylococcal nuclease is accompanied by local unfolding of the protein and/or a substantial penetration of water.[95] The main problem is to capture this change in configuration within practical simulation times. This proved to be a major challenge for microscopic calculations,[96,97] which gave a very large deviation from the observed pK_a values of around 20 pK_a units.[95]

Additional spectroscopic (NMR, EPR, ESR) and isotope-labelling investigations would be of foremost benefit to confirm or disprove the mechanism proposed in our study. From the computational point of view it remains a major challenge, beside the use of QM/MM methodology, to calculate H/D nuclear quantum effects by quantization of nuclear motion.[98] All these efforts might result in deeper understanding of the catalytic steps and the inhibition reactions of MAO and other flavoenzymes, and ultimately in the design and the synthesis of new effective inhibitors.

Acknowledgments

Financial support from the Slovenian Research Agency through Grants P1-0012 and J1-2014 is gratefully acknowledged. R. V. wishes to thank the European Commission for an individual FP7 Marie Curie Intra-European Fellowship for the Career Development, contract number PIEF-GA-2009-255038.

[1] *Monoamine Oxidases – New Vistas* (Eds.: E. Costa, M. Sandler), Reven Press, New York, **1972**.
[2] F. Müller, *Chemistry and Biochemistry of Flavoenzymes*, vol. 3, CRC Press, Boca Raton, **1992**.
[3] M. W. Fraaije, A. Mattevi, *Trends Biochem. Sci.* **2000**, *25*, 126–132.
[4] V. Joosten, W. J. H. van Berkel, *Curr. Opin. Chem. Biol.* **2007**, *11*, 195–202.
[5] M. H. Hefti, J. Vervoort, W. J. H. van Berkel, *Eur. J. Biochem.* **2003**, *270*, 4227–4242.
[6] H.-F. Wu, K. Chen, J. C. Shih, *Mol. Pharmacol.* **1993**, *43*, 888–893.
[7] R. K. Nandigama, D. E. Edmondson, *J. Biol. Chem.* **2000**, *275*, 20527–20532.
[8] J. P. Johnston, *Biochem. Pharmacol.* **1968**, *17*, 1285–1297.
[9] J. Knoll, K. Magyar, *Adv. Biochem. Psychopharmacol.* **1972**, *5*, 393–408.
[10] G. J. Siegel, *Basic neurochemistry: molecular, cellular, and medical aspects*, Elsevier, Amsterdam, Boston, 7th ed., **2006**.
[11] K. N. Westlund, in: *Monoamine oxidase inhibitors in neurological diseases* (Ed.: A. N. Lieberman), CRC Press, **1994**, pp. 1–20.
[12] T. Wichmann, M. R. DeLong, in: *Basic Neurochemistry: Molecular, Cellular and Medical Aspects*, 7th ed. (Eds.: G. Siegel, R. W. Albers, S. Brady, D. Price), Elsevier, New York, **2006**, pp. 887–909.
[13] M. B. Youdim, D. Edmondson, K. F. Tipton, *Nat. Rev. Neurosci.* **2006**, *7*, 295–309.
[14] V. Glover, M. Sandler, F. Owen, G. J. Riley, *Nature* **1977**, *265*, 80–81.
[15] S. G. Waxman, in: *Clinical Neuroanatomy* (Ed.: S. G. Waxman), McGraw Hill, New York, **2010**, pp. 183–194.
[16] National Collaborating Centre for Chronic Conditions *(NCCCC)*, *Parkinson's disease: National clinical guideline for diagnosis and management in primary and secondary care*, National Collaborating Centre for Chronic Conditions, Royal College of Physicians, London, **2006**.
[17] T. Wichmann, M. R. DeLong, in: *Basic Neurochemistry: Molecular, Cellular and Medical Aspects*, 7th ed., (Eds.: G. Siegel, R. W. Albers, S. Brady, D. Price), Elsevier, New York, **2006**, pp. 761–790.
[18] M. Horstink, E. Tolosa, U. Bonuccelli, G. Deuschl, A. Friedman, P. Kanovsky, J. P. Larsen, A. Lees, W. Oertel, W. Poewe, O. Rascol, C. Sampaio, *Eur. J. Neurol.* **2006**, *13*, 1186–1202.
[19] L. S. Goodman, L. L. Brunton, B. Chabner, B. C. Knollmann, *Goodman & Gilman's pharmacological basis of therapeutics*, McGraw-Hill, New York, 12th edn., **2011**.
[20] C. Binda, F. Hubalek, M. Li, D. E. Edmondson, A. Mattevi, *FEBS Lett.* **2004**, *564*, 225–228.
[21] C. Binda, F. Hubalek, M. Li, Y. Herzig, J. Sterling, D. E. Edmondson, A. Mattevi, *J. Med. Chem.* **2004**, *47*, 1767–1774.
[22] M. Li, C. Binda, A. Mattevi, D. E. Edmondson, *Biochemistry* **2006**, *45*, 4775–4784.
[23] D. E. Edmondson, C. Binda, A. Mattevi, *Arch. Biochem. Biophys.* **2007**, *464*, 269–276.
[24] M. A. Akyüz, S. S. Erdem, D. E. Edmondson, *J. Neural Transm.* **2007**, *114*, 693–698.
[25] L. De Colibus, M. Li, C. Binda, A. Lustig, D. E. Edmondson, A. Mattevi, *Proc. Natl. Acad. Sci. USA* **2005**, *102*, 12684–12689.
[26] C. Binda, P. Newton-Vinson, F. Hubalek, D. E. Edmondson, A. Mattevi, *Nat. Struct. Biol.* **2002**, *9*, 22–26.
[27] S. Y. Son, J. Ma, Y. Kondou, M. Yoshimura, E. Yamashita, T. Tsukihara, *Proc. Natl. Acad. Sci. USA* **2008**, *105*, 5739–5744.
[28] S. S. Erdem, O. Karahan, I. Yildiz, K. Yelekci, *Org. Biomol. Chem.* **2006**, *4*, 646–658.
[29] C. Binda, J. Wang, M. Li, F. Hubálek, A. Mattevi, D. E. Edmondson, *Biochemistry* **2008**, *47*, 5616–5625.
[30] J. P. Klinman, D. Mu, *Annu. Rev. Biochem.* **1994**, *63*, 299–344.
[31] E. C. Ralph, J. S. Hirschi, M. A. Anderson, W. W. Cleland, D. A. Singleton, P. F. Fitzpatrick, *Biochemistry* **2007**, *46*, 7655–7664.
[32] K. Csiszar, *Prog. Nucleic Acid Res. Mol. Biol.* **2001**, *70*, 1–32.
[33] M. S. Pilone, *Cell Mol. Life Sci.* **2000**, *57*, 1732–1747.
[34] M. F. Reid, C. A. Fewson, *Crit. Rev. Microbiol.* **1994**, *20*, 13–56.

[35] W. Kroutil, H. Mang, K. Edegger, K. Faber, *Adv. Synth. Catal.* **2004**, *346*, 125–142.
[36] J. R. Miller, D. E. Edmondson, *Biochemistry* **1999**, *38*, 13670–13683.
[37] R. B. Silverman, X. Lu, J. J. P. Zhou, A. Swihart, *J. Am. Chem. Soc.* **1994**, *116*, 11590–11591.
[38] R. B. Silverman, X. Lu, *J. Am. Chem. Soc.* **1994**, *116*, 4129–4130.
[39] R. B. Silverman, *Acc. Chem. Res.* **1995**, *28*, 335–342, and references cited therein.
[40] R. B. Silverman, *Prog. Brain Res.* **1995**, *106*, 23–31.
[41] R. B. Silverman, *J. Biol. Chem.* **1983**, *258*, 14766–14769.
[42] R. B. Silverman, *Biochem. Soc. Trans.* **1991**, *19*, 201–206.
[43] R. B. Silverman, C. K. Hiebert, *Biochemistry* **1988**, *27*, 8448–8453.
[44] R. B. Silverman, R. B. Yamasaki, *Biochemistry* **1984**, *23*, 1322–1332.
[45] D. E. Edmondson, C. Binda, J. Wang, A. K. Upadhyay, A. Mattevi, *Biochemistry* **2009**, *48*, 4220–4230.
[46] A. Tan, M. D. Glantz, L. H. Piette, K. T. Yasunobu, *Biochem. Biophys. Res. Commun.* **1983**, *117*, 517–523.
[47] M. Husain, D. E. Edmondson, T. P. Singer, *Biochemistry* **1982**, *21*, 595–600.
[48] R. K. Nandigama, D. E. Edmondson, *Biochemistry* **2000**, *39*, 15258–15265.
[49] J. R. Miller, D. E. Edmondson, C. B. Grissom, *J. Am. Chem. Soc.* **1995**, *117*, 7830–7831.
[50] A. Warshel, *Computer Modeling of Chemical Reactions in Enzymes and Solutions*, Wiley-Interscience, New York, **1997**.
[51] M. C. Walker, D. E. Edmondson, *Biochemistry* **1994**, *33*, 7088–7098.
[52] M. Li, F. Hubalek, P. Newton-Vinson, D. E. Edmondson, *Protein Expression Purif.* **2002**, *24*, 152–162.
[53] R. K. Nandigama, D. E. Edmondson, *Biochemistry* **2000**, *39*, 15258–15265.
[54] J. G. Hardman, L. E. Limbird, A. G. Gilman, *Goodman & Gilman's The Pharmacological Basis of Therapeutics*, Eleventh Edition, McGraw-Hill: New York, **2005**.
[55] H. P. Rang, M. M. Dale, J. M. Ritter, R. J. Flower, *Rang & Dale's Pharmacology*, 6th ed., Churchill Livingstone, Philadelphia, USA, **2007**.
[56] D. Bonivento, E. M. Milczek, G. R. McDonald, C. Binda, A. Holt, D. E. Edmondson, A. Mattevi, *J. Biol. Chem.* **2010**, *285*, 36849–36856.
[57] C. Binda, F. Hubálek, M. Li, Y. Herzig, J. Sterling, D. E. Edmondson, A. Matevi, *J. Med. Chem.* **2005**, *48*, 8148–8154.
[58] L. De Colibus, M. Li, C. Binda, A. Lustig, D. E. Edmondson, A. Mattevi, *Proc. Natl. Acad. Sci. USA* **2005**, *102*, 12684–12689.
[59] C. Binda, M. Li, F. Hubálek, N. Restelli, D. E. Edmondson, A. Mattevi, *Proc. Natl. Acad. Sci. USA* **2003**, *100*, 9750–9755.
[60] A. L. Maycock, R. H. Abeles, J. I. Salach, T. P. Singer, *Biochemistry* **1976**, *15*, 114–125.
[61] C. Binda, M. Li, F. Hubálek, N. Restelli, D. E. Edmondson, A. Mattevi, *Proc. Natl. Acad. Sci. USA* **2003**, *100*, 9750–9755.
[62] F. Hubálek, C. Binda, M. Li, Y. Herzig, J. Sterling, M. B. Youdim, A. Mattevi, D. E. Edmondson, *J. Med. Chem.* **2004**, *47*, 1760–1766.
[63] S. Nakai, F. Yoneda, T. Yamabe, K. Fukui, *Theor. Chem. Acc.* **1999**, *102*, 147–160.
[64] J. P. Foster, F. Weinhold, *J. Am. Chem. Soc.* **1980**, *102*, 7211–7218.
[65] A. D. Boese, J. M. L. Martin, *J. Chem. Phys.* **2004**, *121*, 3405–3416.
[66] a) V. Barone, M. Cossi, *J. Phys. Chem. A* **1998**, *102*, 1995; b) M. Cossi, N. Rega, G. Scalmani, V. Barone, *J. Comput. Chem.* **2003**, *24*, 669.
[67] P. Georgieva, F. Himo, *J. Comput. Chem.* **2010**, *31*, 1707–1714, and references cited therein.
[68] F. Himo, P. E. M. Siegbahn, *Chem. Rev.* **2003**, *103*, 2421–2456.
[69] M. J. Frisch, G. W. Trucks, H. B. Schlegel, G. E. Scuseria, M. A. Robb, J. R. Cheeseman, G. Scalmani, V. Barone, B. Mennucci, G. A. Petersson, H. Nakatsuji, M. Caricato, X. Li, H. P. Hratchian, A. F. Izmaylov, J. Bloino, G. Zheng, J. L. Sonnenberg, M. Hada, M. Ehara, K. Toyota, R. Fukuda, J. Hasegawa, M. Ishida, T. Nakajima, Y. Honda, O. Kitao, H. Nakai, T. Vreven, J. A. Montgomery Jr., J. E. Peralta, F. Ogliaro, M. Bearpark, J. J. Heyd, E. Brothers, K. N. Kudin, V. N. Staroverov, R. Kobayashi, J. Normand, K. Raghavachari, A. Rendell, J. C. Burant, S. S. Iyengar, J. Tomasi, M. Cossi, N. Rega, J. M. Millam, M. Klene, J. E. Knox, J. B. Cross, V. Bakken, C. Adamo, J. Jaramillo, R. Gomperts, R. E. Stratmann, O. Yazyev, A. J. Austin, R. Cammi, C. Pomelli, J. W. Ochterski, R. L. Martin, K. Morokuma, V. G. Zakrzewski, G. A. Voth, P. Salvador, J. J. Dannenberg, S. Dapprich, A. D. Daniels, Ö. Farkas, J. B. Foresman, J. V. Ortiz, J. Cioslowski, D. J. Fox, *Gaussian 09*, revision A.1, Gaussian, Inc., Wallingford CT, **2009**.
[70] S. E. J. Rigby, R. M. G. Hynson, R. R. Ramsay, A. W. Munro, N. S. Scrutton, *J. Biol. Chem.* **2005**, *280*, 4627–4631.
[71] C. W. M. Kay, H. El Mkami, G. Molla, L. Pollegioni, R. R. Ramsay, *J. Am. Chem. Soc.* **2007**, *129*, 16091–16097.
[72] G. M. Sandala, D. M. Smith, L. Radom, *Acc. Chem. Res.* **2010**, *43*, 642–651 and references cited therein.
[73] D. M. Smith, B. T. Golding, L. Radom, *J. Am. Chem. Soc.* **2001**, *123*, 1664–1675.
[74] J. Stubbe, W. A. van der Donk, *Chem. Rev.* **1998**, *98*, 705–762.
[75] M. H. V. Huynh, T. J. Meyer, *Chem. Rev.* **2007**, *107*, 5004–5064.
[76] M. Cordes, B. Giese, *Chem. Soc. Rev.* **2009**, *38*, 892–901.
[77] S. E. Rigby, P. Heathcote, M. C. Evans, J. H. Nugent, *Biochemistry* **1995**, *34*, 12075–12081.
[78] K. P. Beckerman, H. W. Rogers, J. A. Corbett, R. D. Schreiber, M. L. McDaniel, E. R. Unanue, *J. Immunol.* **1993**, *150*, 888–895.
[79] I. V. Tokmakov, M. C. Lin, *J. Am. Chem. Soc.* **2003**, *125*, 11397–11408.
[80] G. T. Yu, Y. H. Ding, X. R. Huang, C. C. Sun, *J. Phys. Chem. A* **2005**, *109*, 1594–1602.
[81] X. S. Tang, M. Zheng, D. A. Chisholm, G. C. Dismukes, B. A. Diner, *Biochemistry* **1996**, *35*, 1475–1484.
[82] S. Soorkia, A. J. Trevitt, T. M. Selby, D. L. Osborn, C. A. Taatjes, K. R. Wilson, S. R. Leone, *J. Phys. Chem. A* **2010**, *114*, 3340–3354.
[83] D. W. Rogers, N. Matsunaga, A. A. Zavitsas, *J. Org. Chem.* **2006**, *71*, 2214–2219.
[84] P. Riesz, T. Kondo, A. J. Carmichael, *Free Radical Res. Commun.* **1993**, *19 Suppl 1*, S45–53.
[85] C. Rajadurai, V. Enkelmann, G. Zoppellaro, M. Baumgarten, *J. Phys. Chem. B* **2007**, *111*, 4327–4334.
[86] J. Qu, T. Katsumata, M. Satoh, J. Wada, J. Igarashi, K. Mizoguchi, T. Masuda, *Eur. J. Inorg. Chem.* **2007**, *13*, 7965–7973.
[87] C. Puzzarini, A. Gambi, *J. Chem. Phys.* **2005**, *122*, 064316.
[88] I. Perez-Juste, L. Carballeira, *J. Chem. Phys.* **2007**, *127*, 164303.
[89] W. F. Nieuwenhuizen, J. H. van Lenthe, E. J. Blomsma, A. C. Van der Kerk-Van Hoof, G. A. Veldink, J. F. Vliegenthart, *Free Radical Res. Commun.* **1997**, *22*, 1101–1108.
[90] C. W. Kay, R. Feicht, K. Schulz, P. Sadewater, A. Sancar, A. Bacher, K. Mobius, G. Richter, S. Weber, *Biochemistry* **1999**, *38*, 16740–16748.
[91] J. C. Guillemin, T. Janati, L. Lassalle, *Adv. Space. Res.* **1995**, *16*, 85–92.
[92] S. S. Erdem, B. Büyükmenekşe, *J. Neural Transm.* **2011**, *118*, 1021–1029.
[93] *Quantum Medicinal Chemistry* (Eds.: P. Carloni, F. Alber), Wiley-VCH, Weinheim, Germany, **2003**.
[94] P. Carloni, U. Röthlisberger, M. Parrinello, *Acc. Chem. Res.* **2002**, *35*, 455–464.
[95] M. Kato, A. Warshel, *J. Phys. Chem. B* **2006**, *110*, 11566–11570.

[96] J. J. Dwyer, A. G. Gittis, D. A. Karp, E. E. Lattman, D. S. Spencer, W. E. Stites, E. B. Garcia-Moreno, *Biophys. J.* **2000**, *79*, 1610–1620.
[97] C. A. Fitch, D. A. Karp, K. K. Lee, W. E. Stites, E. E. Lattman, E. B. Garcia-Moreno, *Biophys. J.* **2002**, *82*, 3289–3304.
[98] S. C. L. Kamerlin, J. Mavri, A. Warshel, *FEBS Lett.* **2010**, *584*, 2759–2766.

Received: June 15, 2011
Published Online: September 29, 2011

